LBL-19759
Preprint c.2

Lawrence Berkeley Laboratory

UNIVERSITY OF CALIFORNIA

LIBRARY AND
DOCUMENTS SECTION

Materials & Molecular Research Division

Submitted to Journal of the Electrochemical Society

CURRENT OSCILLATIONS OBSERVED WITHIN THE LIMITING-CURRENT PLATEAU FOR IRON IN SULFURIC ACID

P. Russell and J. Newman

June 1985

TWO-WEEK LOAN COPY
This is a Library Circulating Copy
which may be borrowed for two weeks.

Prepared for the U.S. Department of Energy under Contract DE-AC03-76SF00098

LBL-19759 c.2

DISCLAIMER

This document was prepared as an account of work sponsored by the United States Government. While this document is believed to contain correct information, neither the United States Government nor any agency thereof, nor the Regents of the University of California, nor any of their employees, makes any warranty, express or implied, or assumes any legal responsibility for the accuracy, completeness, or usefulness of any information, apparatus, product, or process disclosed, or represents that its use would not infringe privately owned rights. Reference herein to any specific commercial product, process, or service by its trade name, trademark, manufacturer, or otherwise, does not necessarily constitute or imply its endorsement, recommendation, or favoring by the United States Government or any agency thereof, or the Regents of the University of California. The views and opinions of authors expressed herein do not necessarily state or reflect those of the United States Government or any agency thereof or the Regents of the University of California.

LBL-19759

Current Oscillations Observed within the Limiting-Current Plateau for Iron in Sulfuric Acid

Philip Russell[1,*] and John Newman[*]

Materials and Molecular Research Division,
Lawrence Berkeley Laboratory, and
Department of Chemical Engineering,
University of California, Berkeley, California 94720

June, 1985

Abstract

The anodic polarization curve for iron rotating-disk electrodes in acidic sulfate electrolytes displays a limiting-current plateau. Sustained current oscillations are observed when the system is potentiostated within a certain potential range on this limiting-current plateau. The frequency of oscillations is found to be proportional to the square root of the disk-electrode rotation speed. Current oscillations are also observed for a hemispherical rotating electrode. The current-time waveform obtained in one of these experiments displays a harmonic component giving rise to a "beat" phenomenon. Current-time waveforms produced by larger disk electrodes (5 mm diameter) rotating at slower speeds (41.7 rad/s) contain a region of high-frequency noise that is present near the position of minimum current in the overall waveform.

---

[1]Present address: Weyerhaeuser Technology Center, Tacoma, Washington 98477

[*]Electrochemical Society Active Member

Key words: Anode, corrosion, polarization.

Introduction

This paper describes sustained current oscillations that are observed within certain potential regions on the limiting-current plateau for iron rotating disk and hemispherical electrodes in sulfuric acid electrolytes. Before describing the results obtained in this work, a brief summary of previous systems displaying sustained oscillations is presented.

Most cases of oscillations in electrochemical systems are observed during the anodic polarization of certain metals. They are directly connected with the characteristic instability of passivating films, porous or otherwise, under specific conditions.

The first case of periodicity in an electrochemical system was described by Fechner[1] in 1828. It concerned periodic deposition and dissolution of silver on an iron substrate, in an acidic silver nitrate solution. Franck[2] obtained oscillations for iron in 1 N H_2SO_4. Large amplitude current fluctuations were obtained when the iron electrode was held at a constant potential of +0.49 V with respect to a normal hydrogen electrode. The electrolyte was stagnant.

Podesta *et al.*[3] have studied the effects of electrolyte convection on oscillations in the iron-sulfuric acid system. Cooper and Bartlett,[4] Landolt *et al.*,[5] and Kinoshita *et al.*[6] have studied oscillations for copper electrodes in various electrolytes. Landolt *et al.*[5] observed oscillations for copper cathodes during the evolution of hydrogen.

Details of other experimental studies are found in a review by Wojtowicz.[7]

The oscillations reported here are unique for two reasons: (1) there is evidence of instability at a certain point in the current cycle, and (2) a harmonic, or beat, phenomenon was observed in the current waveform during one experiment.

Experimental

Three rotating disk electrodes were used in this study. The fabrication of these electrodes has been described previously.[8] In addition, a rotating hemispherical electrode was also studied. The radius and active area of each of these electrodes are given in Table 1.

Three different electrolytes were used. The composition and the pH of each electrolyte are listed in Table 2. The experimental equipment and setup have been described previously.[8]

The procedure used to determine the limiting current revealed a region in the plateau in which current oscillations are observed. Figure 1 is a

Table 1.

Values of the radius and active area for each electrode.

Electrode	Radius [cm]	Active Area [cm^2]
A	0.247	0.192
B	0.149	0.0697
C	0.0493	0.00764
Hemi	0.197	0.244

Table 2.

Compositions of the electrolytic solutions.

Electrolyte	H_2SO_4 (M)	Na_2SO_4 (M)	Approximate pH
E0	1.0	0.0	0.35
E1	0.288	0.712	1.0
E2	0.0476	0.952	2.0

qualitative sketch illustrating the potential region, ΔV_{osc}, in which current oscillations are observed. To record current oscillations, the potential is increased from V_{oc} to point A, then reversed to a sampling voltage, V_s, located near the center of ΔV_{osc}. A storage oscilloscope is used to record the current as a function of time.

On the forward voltage sweep from V_{oc} to point A, the region of oscillations is not observed because of the current overshoot-undershoot phenomenon. The solid line in Figure 2 is representative of the typical current *vs.* potential behavior observed on the forward sweep. Epelboin *et al.*[9] claim the current overshoot is an experimental artifact due to the finite voltage sweeprate. Beck[10] attributes it to the formation and structural rearrangement of a ferrous sulfate film on the electrode surface.

The magnitudes of the overshoot above, and the undershoot below the limiting current increase as the voltage sweep rate increases. The overshoot-undershoot phenomenon is not observed for a negative voltage sweep, provided that the current is at the limiting value before the negative sweep begins. Figure 2 illustrates the procedure used to determine the limiting-current plateau and the region of current oscillations. The potential is swept in the positive direction, stopped about 30 mV negative of V_{A-P} (point A), and then reversed in the negative direction. The limiting-current plateau and the region containing the current oscillations (dashed line) may be determined very accurately from this negative sweep, which is free from overshoot-undershoot effects.

The current oscillations cannot be observed if the electrode is allowed to passivate. In the case of passivation, the path indicated by the dotted line in Figure 2 is followed. We illustrate the results obtained for a potentiostat that has a vertical load line. The potential is reversed at point B, and the electrode remains passivated until V_{P-A} is reached. The activation process is

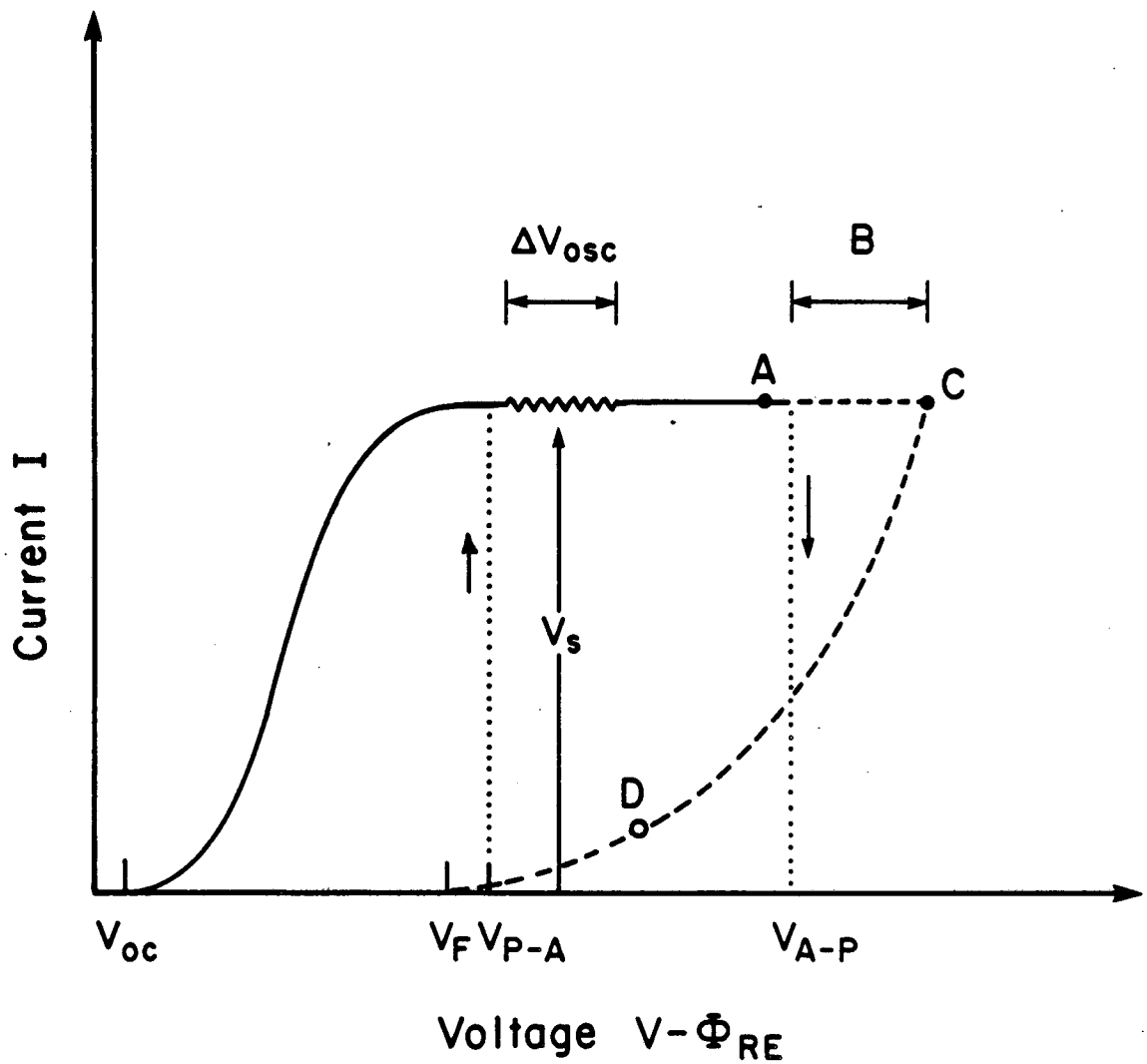

Figure 1. Schematic diagram illustrating the potential region where current oscillations are observed.

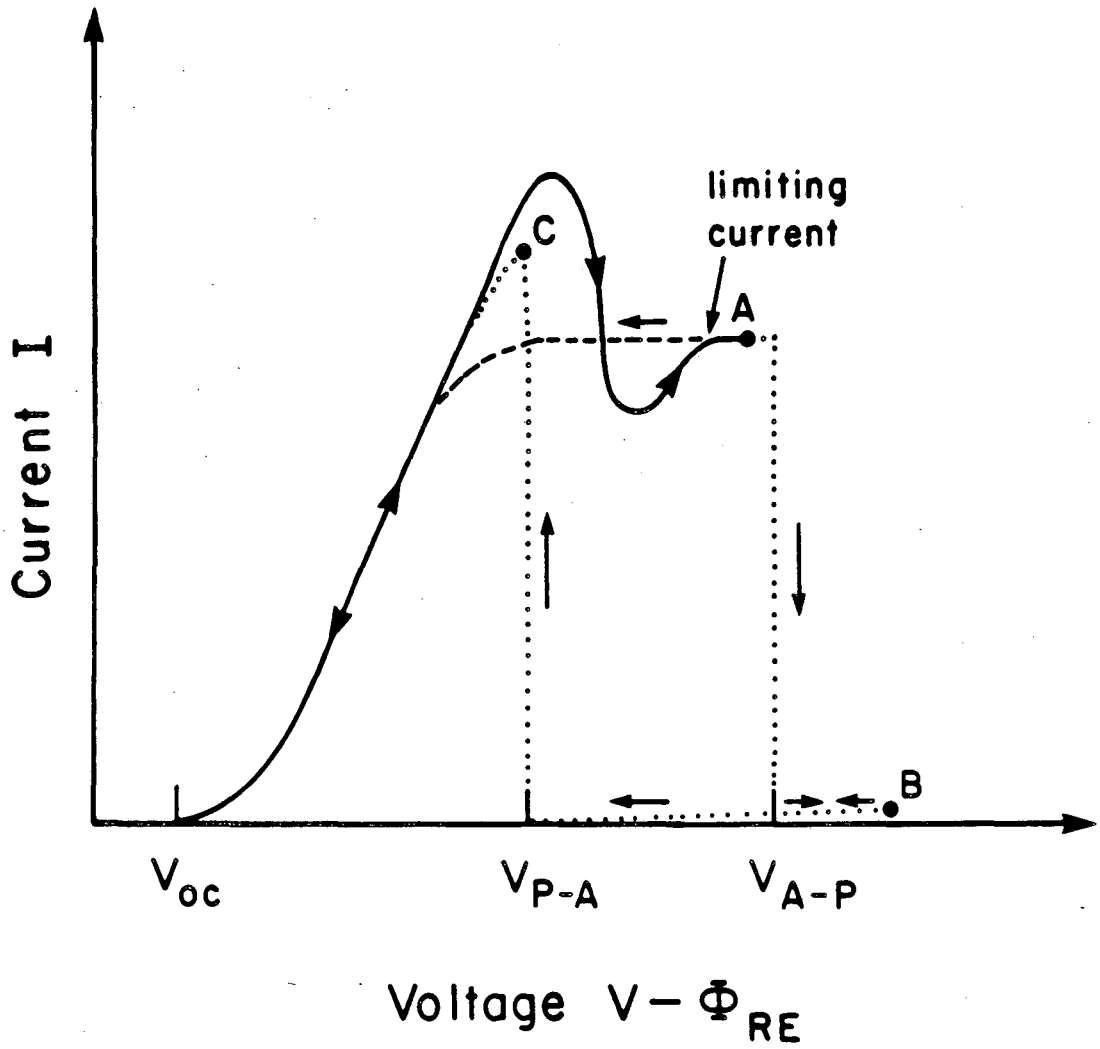

Figure 2. Potentiodynamic sweep results for a typical experiment.

characterized by an overshoot above the limiting current, the current approaching the ohmic limit,[10] as indicated by point C.

When a load line with a positive slope is used, random fluctuations are observed in region B (Figure 1) of the limiting-current plateau, and also on the active-passive transition, line C-D. However, these random fluctuations are strongly dependent on the stability control settings of the potentiostat. At minimum stability, it is not possible to determine the pattern of fluctuations because the potentiostat becomes unstable. At increased stability settings, the current fluctuations in region B can be recorded. The dashed curve in Figure 1 represents the time average of these fluctuations. The oscillations in region B and the active-passive transition persist, even at the maximum stability setting.

The oscillations in the potential range ΔV_{osc} are independent the stability setting on the potentiostat. These oscillations are characteristic of the system itself and not the electronics.

Results and discussion

This paper concerns only current oscillations observed in the region ΔV_{osc} of Figure 1. The oscillations in region B and in the transition curve of Figure 1 are not considered.

All potentials reported in this paper are measured with respect to a mercury-mercurous sulfate, saturated potassium sulfate reference electrode.

Figure 3 is a plot of the potentiodynamic sweep results for electrode B in the E0 electrolyte. The potential range in which oscillations occur is ΔV_{osc}. Potentiostating the system at point A (-0.360 V) at a rotation speed of 41.9 rad/s (400 rpm) results in the sustained current oscillations plotted in Figure 4. The current density (based on total electrode area) is plotted as a function

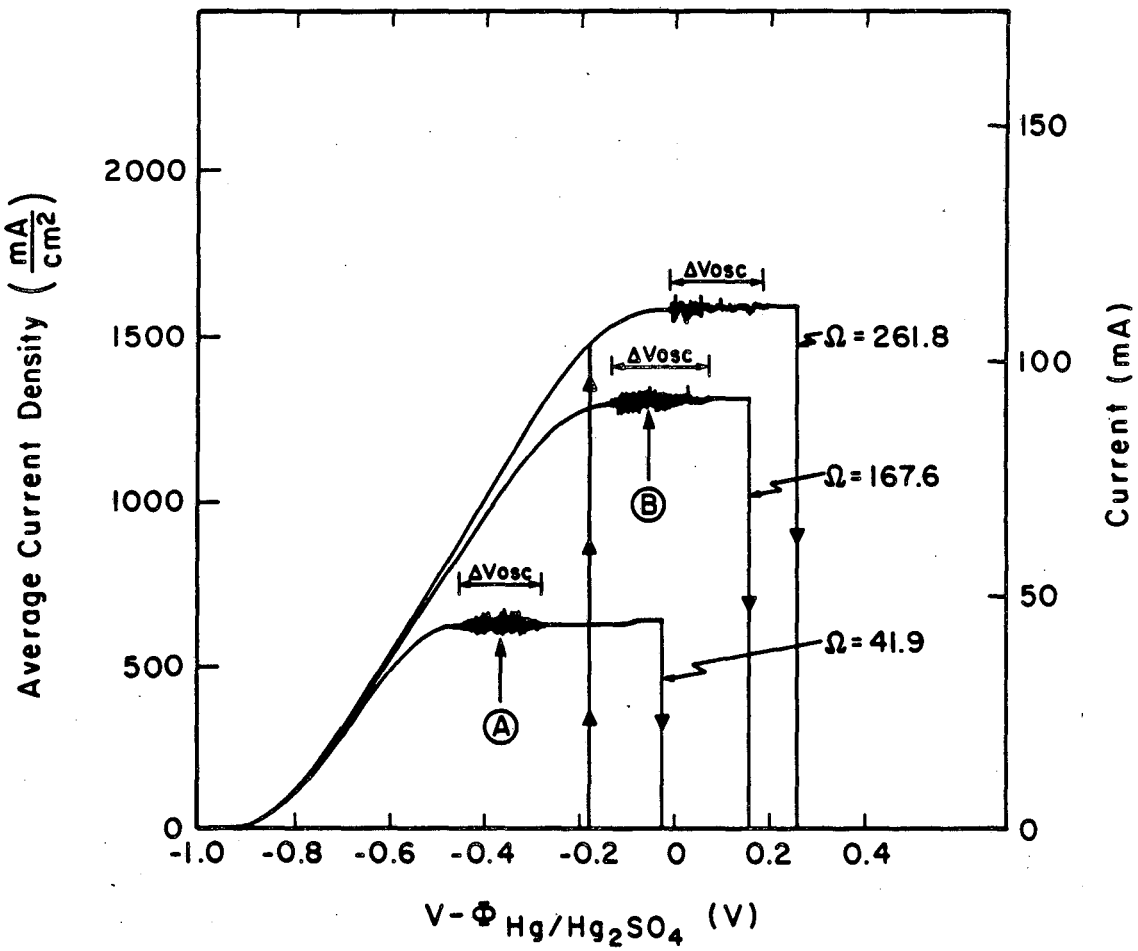

Figure 3. Potentiodynamic sweep curves for electrode B in the E0 electrolyte. Regions in which oscillations are observed are indicated. For clarity, the current overshoot phenomenon is not shown.

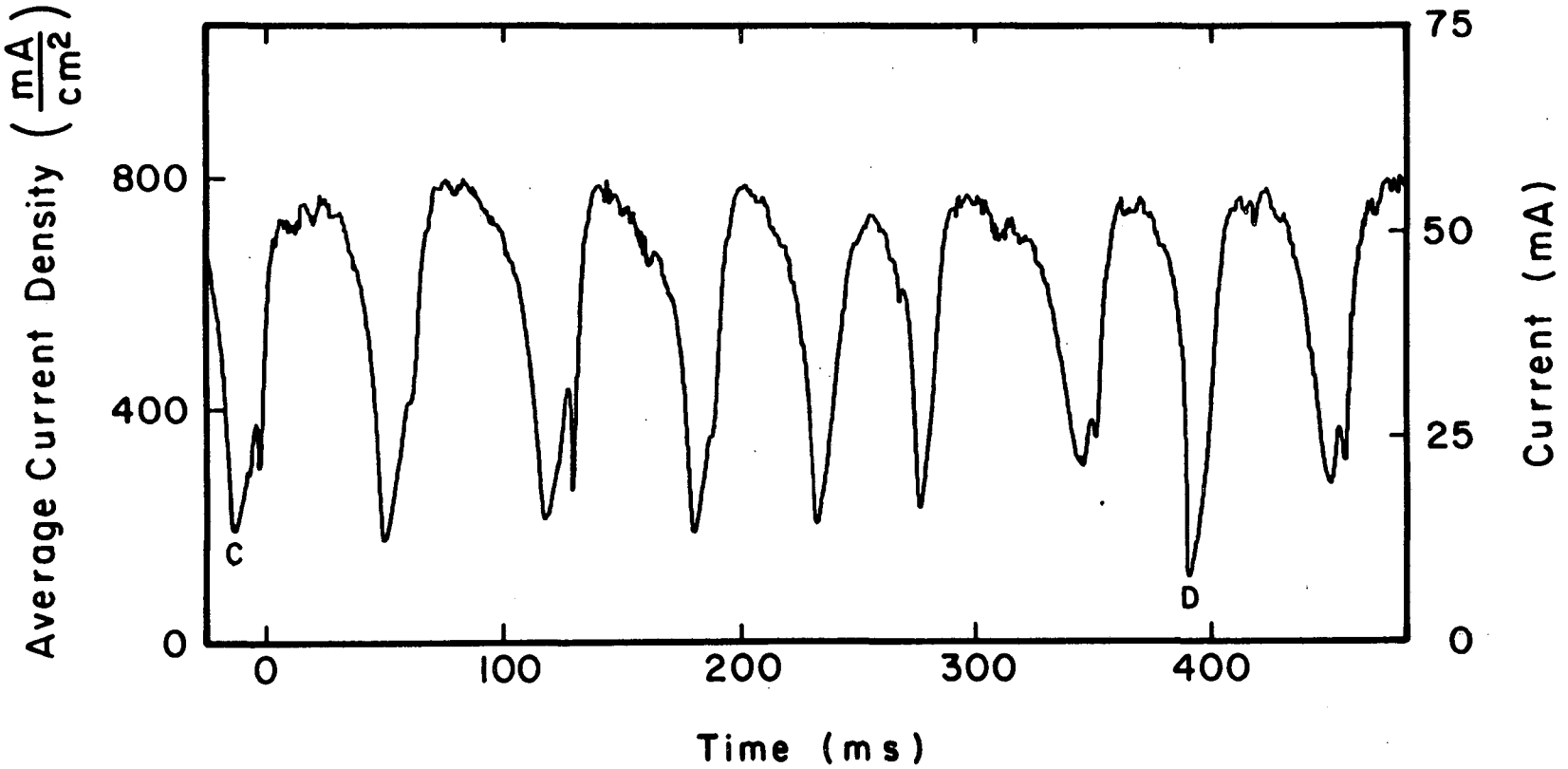

Figure 4. Sustained oscillations observed for electrode B in the E0 electrolyte at Ω = 41.9 rad/s. Electrode is polarized at point A on Figure 3.

of time. The period for each cycle is not uniform. For the seven cycles shown from point C to point D, the average frequency is 17.8 Hz. When 30 cycles (including the 7 shown in Figure 4) are considered, the average frequency is 18.7 Hz.

The total current varies between 15 and 55 mA during the average cycle. The magnitude of these variations is not shown to scale on Figure 3 because the time response of the X-Y recorder is too slow to keep up with the oscillations. The storage oscilloscope recorded the results shown in Figures 4 and 5.

Figure 5 illustrates the current-time behavior for a rotation speed of 167.6 rad/s (1600 rpm). The potential was increased to -0.050 V (point B on Figure 3). The periods of the cycles have significant variations. The shape of each cycle is not uniform. For approximately half the cycles in Figure 5, there is a brief period when the current signal contains significant noise at minimum current. This phenomenon will be examined more closely in the next section.

The frequency of oscillations was found to be proportional to the square root of disk rotation speed. The results for three disk rotation speeds in the EO electrolyte are indicated in Figure 6 by the symbols + and o. The average frequency for each run is plotted as a function of the square root of disk rotation speed. These results are summarized in the first 9 lines of Table 3, where the average frequency of each of the three runs that were carried out at each rotation speed is listed. The frequency of oscillations is nearly independent of electrode size. Podesta *et al.*[3] have studied the effects of disk rotation speed on frequency of oscillations. They investigated a rotation speed range from 15.7 to 41.9 rad/s (150 to 400 rpm). For a constant acid concentration and temperature, the following equation was found to characterize their data

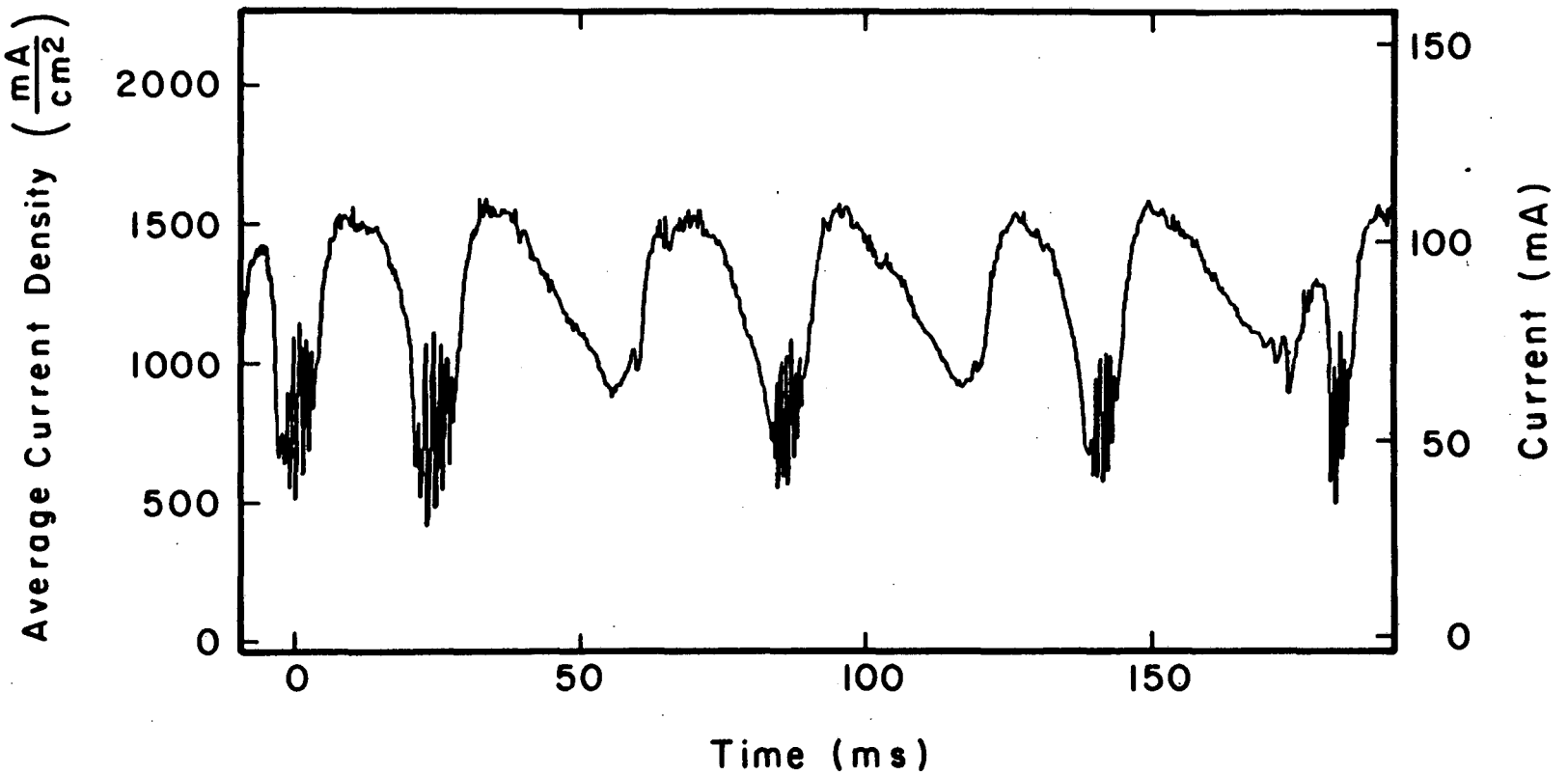

Figure 5. Sustained oscillations observed for electrode B in the E0 electrolyte at Ω = 167.6 rad/s. Electrode is polarized at point B on Figure 3.

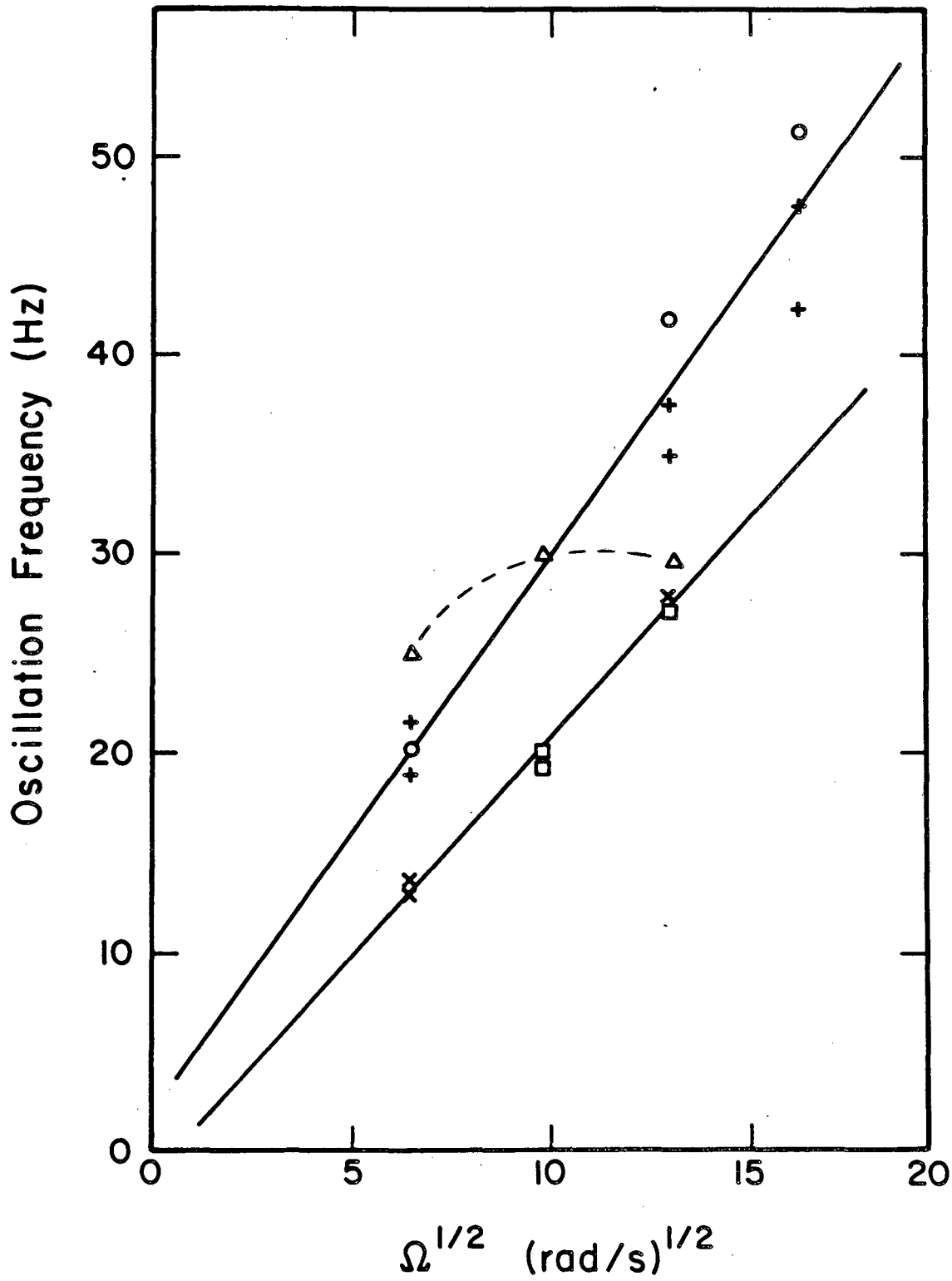

Figure 6. Frequency dependence of oscillations on electrode rotation speed for five systems: o, electrode A in the E0 electrolyte; +, electrode B in the E0 electrolyte; x, electrode B in the E1 electrolyte; □, electrode C in the E1 electrolyte; and Δ, hemisphere electrode in the E0 electrolyte.

Table 3.

Frequencies of oscillations at various rotation speeds.

Rotation Speed [rad/s]	Electrode	Electrolyte	$(V - \Phi_{Hg/Hg_2SO_4})$ [V]	Oscillation Frequency [Hz]
41.9	A	E0	-0.140	20.1
41.9	B	E0	-0.360	18.7
41.9	B	E0	-0.380	21.4
167.6	A	E0	+0.240	41.7
167.6	B	E0	-0.050	34.8
167.6	B	E0	-0.110	37.4
261.8	A	E0	+0.452	51.3
261.8	B	E0	+0.130	42.2
261.8	B	E0	+0.220	47.6
41.9	B	E1	0.000	12.7
41.9	B	E1	-0.050	13.4
94.2	C	E1	-0.265	19.9
94.2	C	E1	-0.265	19.1
167.6	C	E1	-0.150	27.1
167.6	B	E1	+0.628	27.8
41.9	Hemi	E0	-0.270	24.9
94.2	Hemi	E0	-0.110	29.9
167.6	Hemi	E0	-0.060	29.4

$$f = A + B\Omega^{1/2}. \tag{1}$$

A least-squares fit was used to determine the constants in Equation (1) based on the first nine lines in Table 3. The results are: A = 2.08 Hz and B = 2.78 (Hz)(rad/s)$^{-1/2}$. Equation (1) is included in Figure 6 for comparison, and is

shown to be valid to at least 261.8 rad/s (2500 rpm).

Figure 6 also shows the more limited data obtained from electrodes B and C in the E1 electrolyte. Data from the hemispherical electrode in the E0 electrolyte are also plotted in Figure 6. The frequency dependence for the hemisphere is weak compared to the disk.

Current instabilities during periodic oscillations

An example of the current instabilities that were often observed near the position of minimum current during a cycle is shown in Figure 7. The frequency of repetition of the entire wave form is about 20.1 Hz. There is a much faster group of oscillations that is observed near the minimum current position. A clearer picture of these faster oscillations is obtained by increasing the oscilloscope trace speed. The results shown in Figure 8 are obtained under identical conditions as those of Figure 7; the expanded time scale on the abscissa is the only difference. The frequency of the faster current oscillations is approximately 1200 Hz. The large difference in their characteristic times indicates these two processes must have different mechanisms.

No noise was observed for electrode B oscillating at 18.7 Hz in the E0 electrolyte at a rotation speed of 41.9 rad/s (see Figure 4). Noise was observed for electrode A oscillating at 20.1 Hz under the identical conditions, as shown in Figure 7. The overall frequency of oscillations is roughly the same in both cases. The only difference is the larger size of electrode A. This indicates that a larger electrode may be more unstable with respect to jumping between the active and passive states than a smaller electrode. This is analogous to the argument used previously by Russell and Newman[8] to explain the negative shift in V_{P-A} as the electrode is decreased in size (see Figure 5 of reference 8).

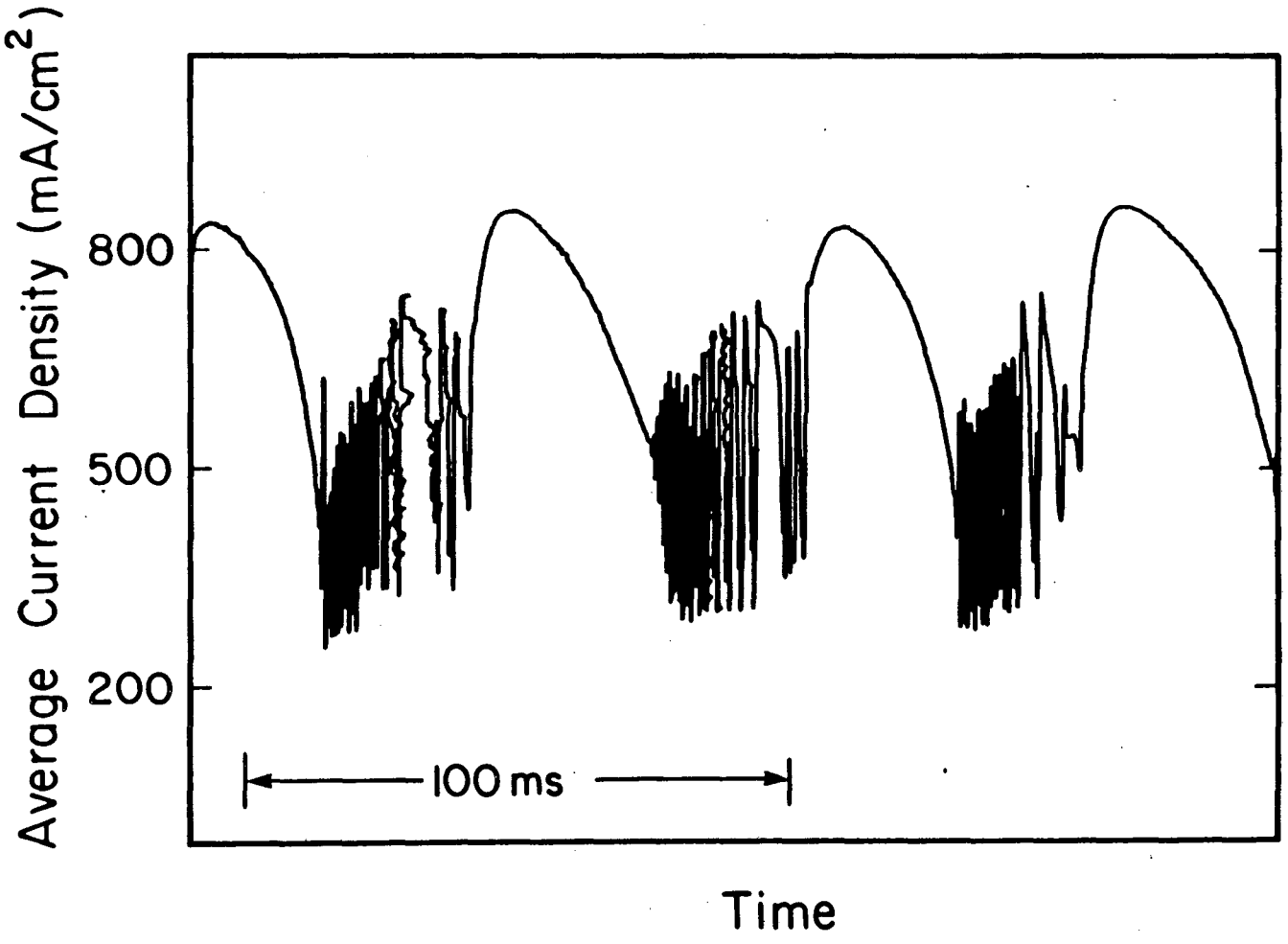

Figure 7. Current-time plot for electrode A, at a potential of -0.140 V and a rotation speed of 41.9 rad/s, in the E0 electrolyte illustrating current instabilities near the position of minimum current.

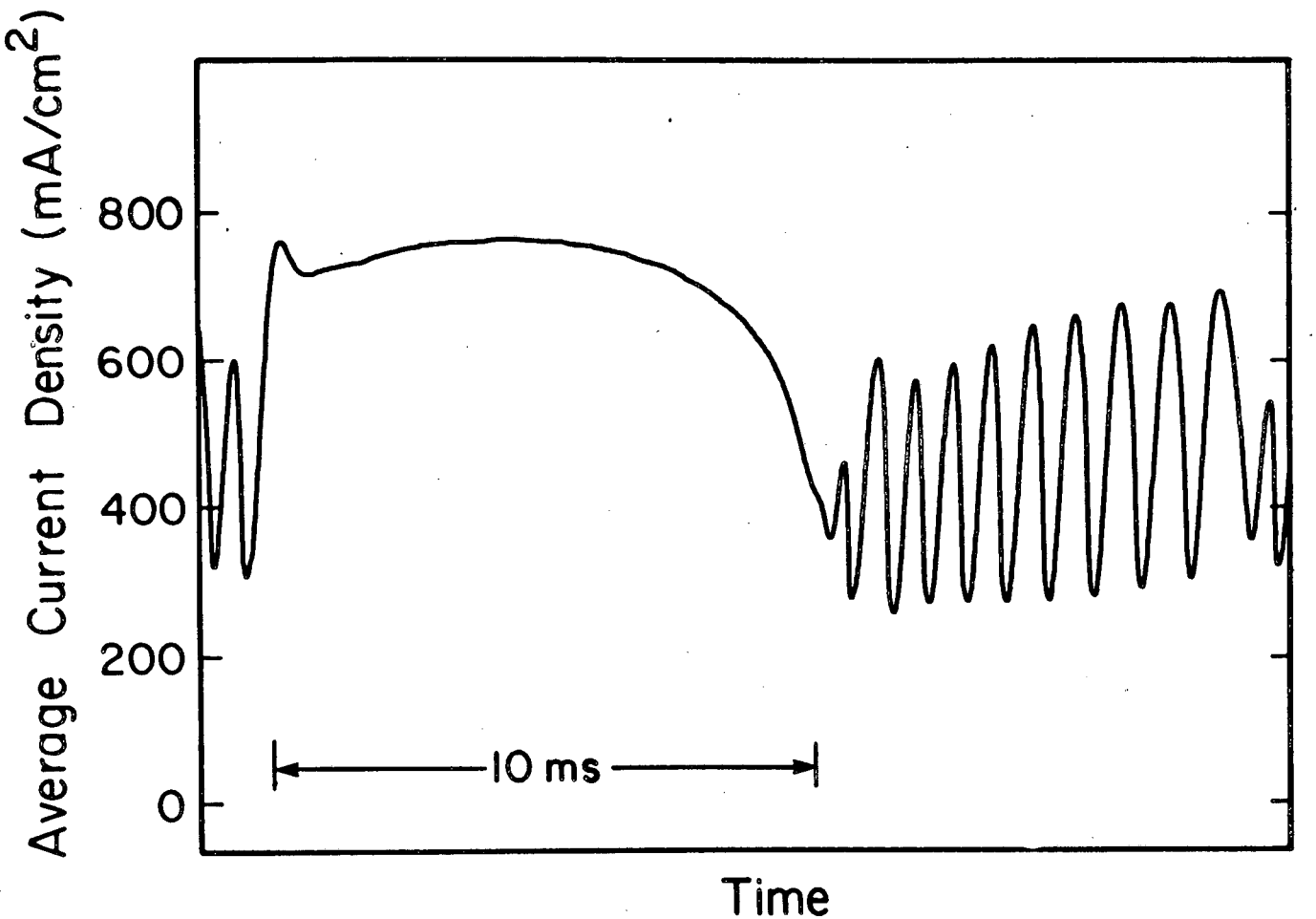

Figure 8. Current-time plot for the same conditions as in Figure 7. The time scale on the abscissa has been expanded to permit a more detailed examination of the current instabilities occurring near minimum current.

Current-time curves for electrode C, at a rotation speed of 377.0 rad/s (3600 rpm), in the E0 electrolyte are presented in Figure 9. These plots are obtained from a single current-time oscilloscope trace. They proceed in chronological order. Figure 9 (a) illustrates a uniform oscillatory pattern. In Figure 9 (b), the peaks can be divided into two groups, A and B. As time increases, the peaks in group A remain nearly constant in size and shape. The peaks in group B are seen to decrease in size and actually become a shoulder to the constant sized peaks. Although it is not illustrated here, the shoulders will grow in time, restoring the uniform pattern of Figure 9 (a). This waveform appears to display a "beat" phenomenon.

Results for the hemispherical electrode

Oscillations are observed for the hemispherical electrode. Figure 10 illustrates typical current-time behavior for a rotation speed of 94.2 rad/s. The results are essentially similar to those seen for the disk electrode. This indicates that the oscillations are not totally dependent on the highly nonuniform potential distribution associated with the disk system. Figure 6 and Table 3 present additional results in a manner that facilitates comparison with the corresponding data from the disk system. It is not clear why the frequency dependence on rotation speed for the hemispherical system is weaker than that for the disk system.

General observations

The width of the region in which oscillations are observed, ΔV_{osc}, increases slightly with increasing rotation speed. This is illustrated in Table 4, where results are tabulated for the hemispherical electrode at various rotation speeds.

The oscillation frequencies reported up to this point have all been obtained at the center of ΔV_{osc}. The frequency of oscillations is relatively

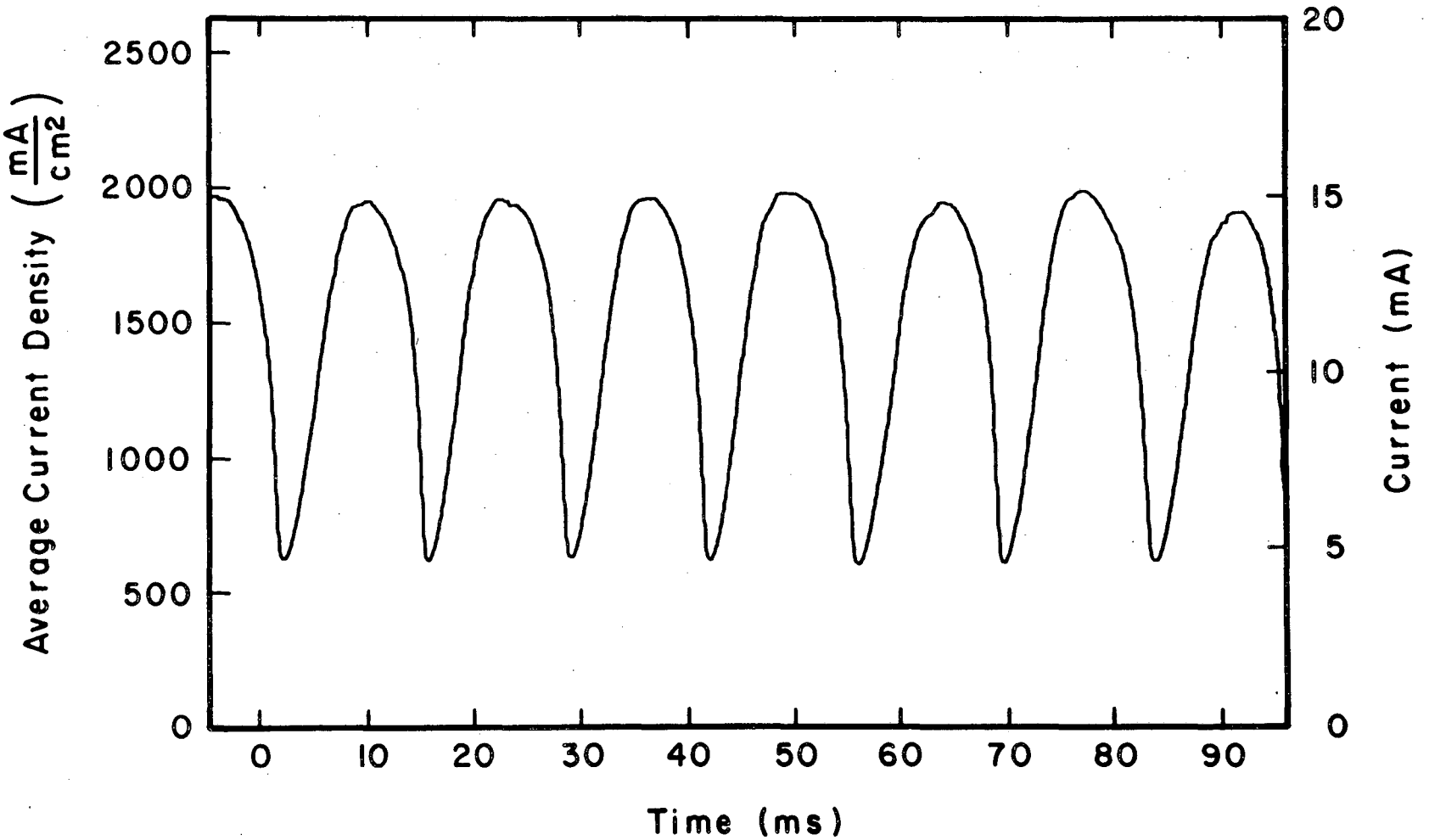

Figure 9 (a). Electrode C for Ω = 377.0 rad/s, V - Φ_{RE} = -0.271 V, in the E0 electrolyte. A uniform oscillatory pattern.

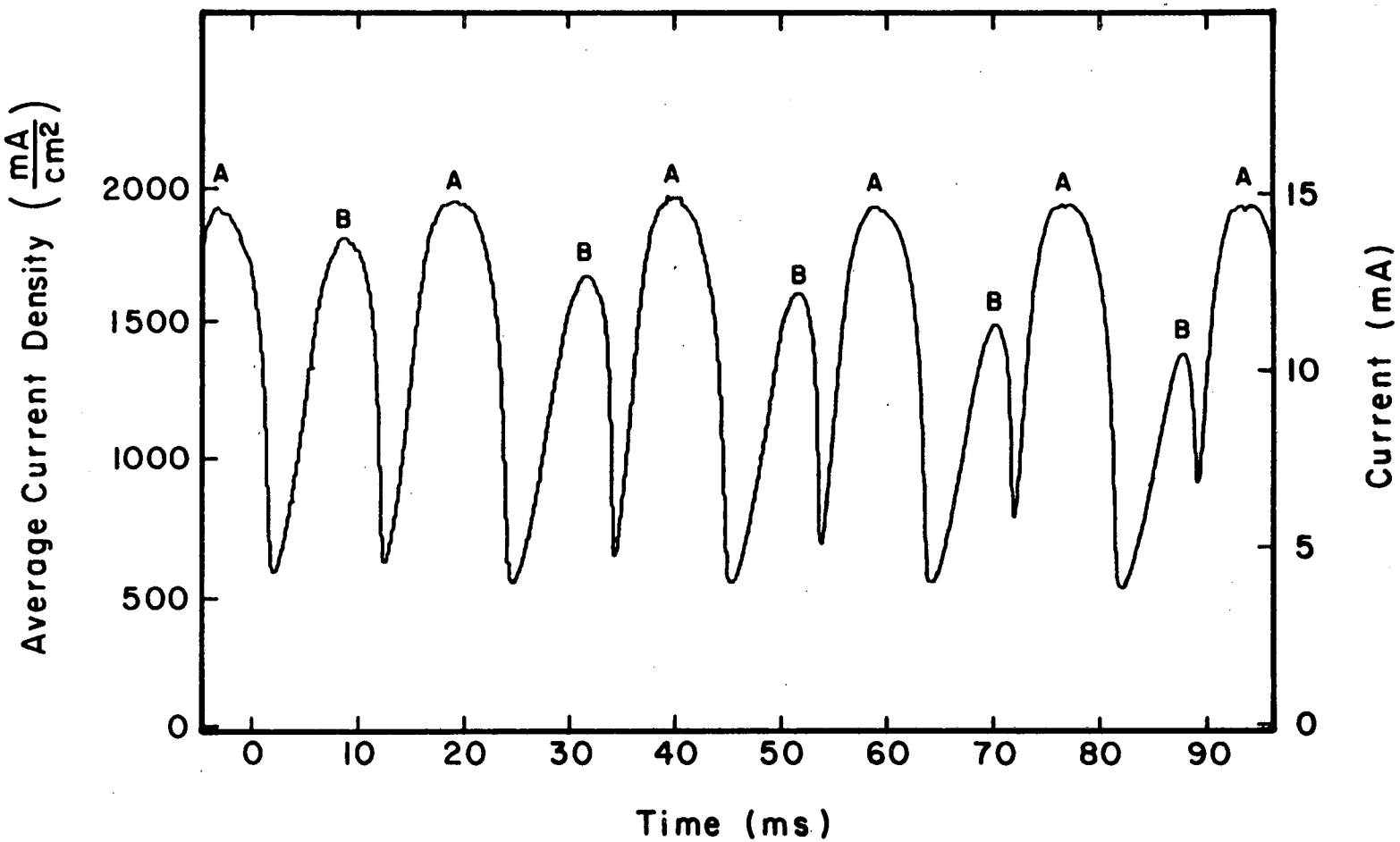

Figure 9 (b). Continuation of the same oscilloscope trace as in (a). Growth of a shoulder in the wave form is illustrated.

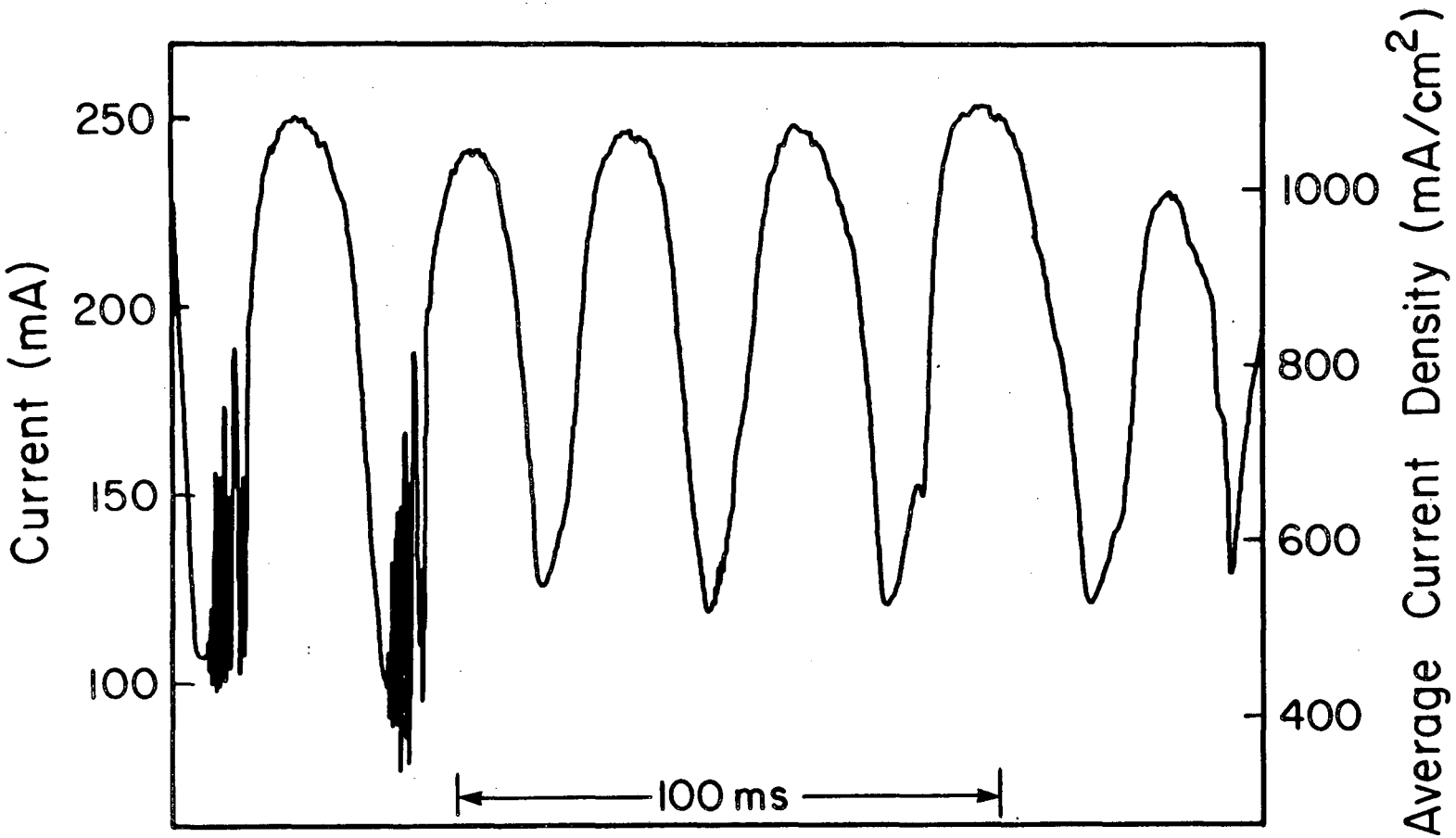

Figure 10. Oscillations observed for the hemisphere electrode in the E0 electrolyte. Ω = 94.2 rad/s, $(V - \Phi_{Hg/Hg_2SO_4})$ = -0.11 V, with an average frequency of 29.9 Hz.

Table 4.

Width of ΔV_{osc} at various rotation speeds

for the hemispherical electrode in the E0 electrolyte.

Ω [rad/s]	$(V - \Phi_{Hg/Hg_2SO_4})$ where oscillations begin [V]	$(V - \Phi_{Hg/Hg_2SO_4})$ where oscillations end [V]	Width of ΔV_{osc} [V]
41.9	-0.35	-0.17	0.18
94.2	-0.23	-0.02	0.21
167.6	-0.15	0.08	0.23

independent of the position within ΔV_{osc}. At Ω = 167.6 rad/s, in the E0 electrolyte, the hemisphere has a ΔV_{osc} of 0.23 V, ranging from -0.15 to 0.08 V (see Table 4). Oscillation frequencies were measured at potentials of -0.12, -0.06, and 0.00 V with results of 25.0, 29.5, and 30.2 Hz, respectively.

Conclusions

(*i*) Both the rotating disk and the rotating hemispherical electrodes displayed continuous oscillations within certain potential ranges on the limiting-current plateau. The frequency of these oscillations is proportional to the square root of rotation speed for the disk electrodes in the E0 electrolyte.

(*ii*) The frequency of oscillations for the hemispherical electrode is more weakly dependent on the electrode rotation speed.

(*iii*) Noise is often observed near the position of minimum current for the sustained oscillations. Increasing the size of the electrode or increasing the rotation speed seems to promote the occurrence of this noise.

(*iv*) The growth of a shoulder followed by its subsequent disappearance was observed in a continuous oscillatory waveform.

Future Work

We have developed a mathematical model describing the formation of a porous salt film on the electrode surface. This model is being extended to show that transient changes in the potential and concentration gradients that develop within the pores of the salt film are sufficient to cause local areas on the electode surface to alternate between the active and the passive states. This alternation between states is responsible for the observed oscillations.

This work will be submitted for publication in the near future.

Acknowledgment

This work was supported by the Assistant Secretary of Conservation and Renewable Energy, Office of Energy Systems Research, Energy Storage Division of the United States Department of Energy under Contract Number DE-AC03-76SF00098.

List of symbols

A	Electrode with diameter of 0.494 cm
B	Electrode with diameter of 0.298 cm
C	Electrode with diameter of 0.0986 cm
E0	1 M H_2SO_4 electrolyte, pH = 0.3
E1	Electrolyte with pH = 1
E2	Electrolyte with pH = 2
f	Oscillation frequency, Hz
V	Electrode potential, V
V_s	Potential where oscillations are recorded, V
V_{oc}	Open circuit potential, V
	Greek letters
ΔV_{osc}	Potential range containing oscillations, V
Φ_{Hg/Hg_2SO_4}	Potential of saturated mercurous sulfate reference electrode, V
Ω	Electrode rotation speed, rad/s

References

1. Fechner. *Schweigg. J.*, **53** (1828), 141.

2. U. F. Franck. "Instabilitäterscheinungen an passivierbaren Metallen." *Zeitschrift für Elektrochemie*, **62** (1958), 649-655.

3. J. J. Podestá, R. C. V. Piatti, and A. J. Arvía. "The Potentiostatic Current Oscillations at Iron/Sulfuric Acid Solution Interfaces." *Journal of the Electrochemical Society*, **126** (1979), 1363-1367.

4. R. S. Cooper and J. H. Bartlett. "Convection and Film Instability: Copper Anodes in Hydrochloric Acid." *Journal of the Electrochemical Society*, **105** (1958), 109-116.

5. Dieter Landolt, Raul Acosta, Rolf H. Muller, and Charles W. Tobias. "An Optical Study of Cathodic Hydrogen Evolution in High-Rate Electrolysis." *Journal of the Electrochemical Society*, **117** (1970), 839-845.

6. K. Kinoshita, D. Landolt, R. H. Muller, and C. W. Tobias. "Stoichiometry of Anodic Copper Dissolution at High Current Densities." *Journal of the Electrochemical Society*, **117** (1970), 1246-1251.

7. J. Wojtowicz. "Oscillatory Behavior in Electrochemical Systems." J. O'M. Bockris and B. Conway, eds. *Modern Aspects of Electrochemistry*, No. **8**, (New York: Plenum Press, 1972), Chapter 2, pp. 47-120.

8. Philip P. Russell and John Newman. "Experimental Determination of the Passive-Active Transition for Iron in 1 *M* Sulfuric Acid." *Journal of the Electrochemical Society*, **130** (1983), 547-553.

9. Israël Epelboin, Claude Gabrielli, Michel Keddam, Jean-Claude Lestrade, and Hisasi Takenouti. "Passivation of Iron in Sulfuric Acid Medium." *Journal of the Electrochemical Society*, **119** (1972), 1632-1637.

10. Theodore R. Beck. "Formation of Salt Films during the Passivation of Iron." *Journal of the Electrochemical Society*, **129** (1982), 2412-2418.

Figure Captions

Figure 1. Schematic diagram illustrating the potential region where current oscillations are observed.

Figure 2. Potentiodynamic sweep results for a typical experiment.

Figure 3. Potentiodynamic sweep curves for electrode B in the E0 electrolyte. Regions in which oscillations are observed are indicated. For clarity, the current overshoot phenomenon is not shown.

Figure 4. Sustained oscillations observed for electrode B in the E0 electrolyte at Ω = 41.9 rad/s. Electrode is polarized at point A on Figure 3.

Figure 5. Sustained oscillations observed for electrode B in the E0 electrolyte at Ω = 167.6 rad/s. Electrode is polarized at point B on Figure 3.

Figure 6. Frequency dependence of oscillations on electrode rotation speed for five systems: o, electrode A in the E0 electrolyte; +, electrode B in the E0 electrolyte; x, electrode B in the E1 electrolyte; □, electrode C in the E1 electrolyte; and Δ, hemisphere electrode in the E0 electrolyte.

Figure 7. Current-time plot for electrode A, at a potential of -0.140 V and a rotation speed of 41.9 rad/s, in the E0 electrolyte illustrating current instabilities near the position of minimum current.

Figure 8. Current-time plot for the same conditions as in Figure 7. The time scale on the abscissa has been expanded to permit a more detailed examination of the current instabilities occurring near minimum current.

Figure 9 (a). Electrode C for Ω = 377.0 rad/s, V - Φ_{RE} = -0.271 V, in the E0 electrolyte. A uniform oscillatory pattern.

Figure 9 (b). Continuation of the same oscilloscope trace as in (a). Growth of a shoulder in the wave form is illustrated.

Figure 10. Oscillations observed for the hemisphere electrode in the E0 electrolyte. Ω = 94.2 rad/s, $(V - \Phi_{Hg/Hg_2SO_4})$ = -0.11 V, with an average frequency of 29.9 Hz.

This report was done with support from the Department of Energy. Any conclusions or opinions expressed in this report represent solely those of the author(s) and not necessarily those of The Regents of the University of California, the Lawrence Berkeley Laboratory or the Department of Energy.

Reference to a company or product name does not imply approval or recommendation of the product by the University of California or the U.S. Department of Energy to the exclusion of others that may be suitable.

LAWRENCE BERKELEY LABORATORY
TECHNICAL INFORMATION DEPARTMENT
UNIVERSITY OF CALIFORNIA
BERKELEY, CALIFORNIA 94720